Self-consistent study of single molecular transistor modulated by transverse field

Self-consistent study of single molecular transistor modulated by transverse field

F. Jiang, Y. X. Zhou, and H. Chen[a)]
Department of Physics, Fudan University, Shanghai 200433, People's Republic of China

R. Note, H. Mizuseki, and Y. Kawazoe
Institute for Materials Research, Tohoku University, Sendai 980-8577, Japan

We use a self-consistent method to study the current of the single molecular transistor modulated by the transverse field in the level of the density functional theory and the nonequilibrium Green function method. The numerical results show that both the polyacene-dithiol molecules and the fused-ring thiophene molecules are the potential high-frequency molecular transistors controlled by the transverse field. The longer molecules of the polyacene-dithiol or the fused-ring thiophene are in favor of realizing the gate-bias controlled molecular transistor. The theoretical results suggest the related experiments. © *2006 American Institute of Physics.* [DOI: 10.1063/1.2337286]

I. INTRODUCTION

Using organic molecules as functional units for electronic apparatus application is an interesting goal of nano-electronic devices.[1,2] The common and important function of these devices is that the current can be controlled effectively. In the last several years, many experimental and theoretical works were carried out to study the transport properties through the single molecules, or even to design the molecular electronic devices.[3–28] At present, people have realized two major approaches to control molecular transport. One is through the conformational change in the molecule, and the other is through the external transverse field to switch the molecule from the "on" state to the "off" state. Many authors have focused their attention on the former one for a long time, and achieved advances.[20–24] Despite the fact that the conformational change in molecules can be performed by using the electric or light fields, its operation frequency is low. Now, the attention is transferred to the latter one due to its high operation frequency. Several experiments have identified its feasibility.[25–27] The π-conjugated organic oligomers and polymers are the subject of considerable research interest in the organic semiconductors. The organic semiconductors can be employed as active layers in the field effect transistors (FETs).[25] The gate-bias controlled molecular transistor is successfully realized experimentally[27] from perylene tetra-carboxylic di-imide (PTCDI), a redox molecule. Recently, the current behavior of the single molecule has received increasing attention. Single organic oligomers such as pentathienoacene (PTA), pentacene, perylene, and so on are all the key objects in the theoretical study. At present, some theoretical works have shed light on the organic molecular transistors controlled by the transverse field.[28–31] In this paper, we use the self-consistent calculation in the study of the molecular-transistor-electrode system controlled by the transverse-field effect (TFE) on the basis of the density functional theory (DFT) and nonequilibrium Green function method.

II. THEORY AND METHODS

The retarded Green function of the molecule is expressed as follows:

$$G_M^R = (E^+ S_M - F_M - \Sigma_1^R - \Sigma_2^R)^{-1}, \tag{1}$$

where S_M and F_M are the overlap matrix and Fock matrix of the molecule part, respectively. $\Sigma_1^R(\Sigma_2^R)$ is the retarded self-energy of the left (right) electrode. It should be emphasized that the Fock matrix is obtained after the density matrix is obtained. The overlap matrix and the two electron integral of the Fock matrix are completed by the standard quantum chemistry software GAUSSIAN03.[35]

The density matrix of the open system is the essential function of the whole self-consistent scheme. It can be achieved by the Keldysh Green function

$$\rho = \int_{-\infty}^{\infty} dE[-iG^<(E)/2\pi], \tag{2}$$

$$-iG^< = G_M^R(F_1\Gamma_1 + F_2\Gamma_2)G_M^A, \tag{3}$$

with the advanced Green function $G^A=(G^R)^\dagger$ and the broadening function of the left (right) lead $\Gamma_1(\Gamma_2)$. The Fermi distribution function of the left (right) lead $F_1(F_2)$ is expressed as $F_i(E)=1/(e^{(E-\mu_i)/kT}+1)$ with $\mu_1=E_F-\frac{1}{2}$ eV and $\mu_2=E_F+\frac{1}{2}$ eV. E_F is the Fermi level of the bulk Au. In our work, E_F is -5.1 eV, which is an adjusted parameter around the negative value of the gold work function (5.31 eV) in fcc structure (111) direction for explaining the shape of the I-V curve in the experimental results.[3,32,33] With $E_F=-5.1$ eV, the density of state (DOS) of the three-dimensional gold lead can be obtained numerically in accord with the first-principles results.[32,34] The transverse field perpendicular to the transport direction is applied by the "field" option of GAUSSIAN03;

[a)]Author to whom correspondence should be addressed. Electronic mail: haochen@fudan.edu.cn
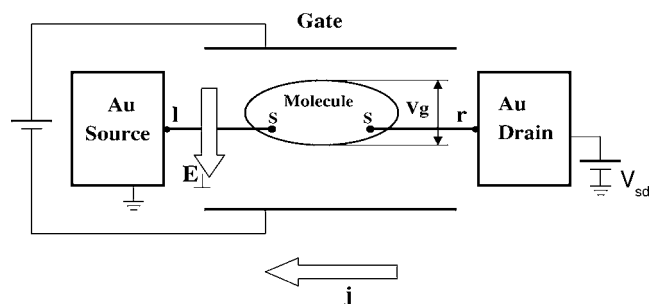
125, 084710-1

FIG. 1. Au lead–molecule–Au lead open system. The molecule chemisorbed to Au source and drain electrodes by sulfur atoms is not symmetric to the S–Au bond. The transverse field is confined inside the molecule region without effect on Au leads and V_g is the gate-bias drop on the molecule.

the corresponding potential energy term is included in the Fock operator.

The molecular device is illustrated in Fig. 1 with the sulfur atom attached by the gold electrode from both sides and both the longitudinal and transverse fields are applied. The potential zero point is set at the coordinate origin, the middle of the line connecting two sulfur atoms, and the whole molecule is not symmetric to the Au–S bond, which will be in favor of TFE. The existence of the transverse field has no effect on the source and drain electrodes. If the potential zero point deviates from this point, the expression of chemical potential of the left and right leads should be rectified: $\mu_1 = E_F - e\left(\frac{1}{2}V + \Delta V\right)$ and $\mu_2 = E_F + e\left(\frac{1}{2}V - \Delta V\right)$, where ΔV is the electrical potential difference between the old zero point and the new one. The choice of the potential zero point has no effect on the calculation results.

The molecule is chemisorbed on the gold contacts by sulfur atoms. The sulfur atom sits on the hollow position of three nearest-neighbor surface gold atoms. The perpendicular distance between the sulfur atom and the gold fcc (111) surface plane is 2.0 Å. The temperature effect is not included for the short molecule in our calculation for simplicity.

The density matrix for the open system is obtained self-consistently by extending the self-consistent calculation for the inner loop in GAUSSIAN03 to the loop composed of the lead-molecule-lead open system under the bias V_{sd} between the source and drain. At the beginning, the self-consistent procedure starts from a guess for the density matrix of the open system, which may be obtained from the converged density matrix of GAUSSIAN03 calculation for the isolated molecule. We feed back the density matrix given by Eq. (2) to the GAUSSIAN's main program as subroutines to obtain the new density matrix. The iterations continue until the density matrix converges to the acceptable accuracy (usually less than 10^{-5}). Then the density matrix is used to evaluate the transmission function (T), the terminal current, the electron number, and DOS of the open system.[32,33] In the calculations, we adopt DFT with B3PW91 exchange-correlation potential and LANL2DZ basis to evaluate the electronic structure and the Fock matrix. The basis set associates with the effective core potential (ECP), which is specially suited for the fifth-row (Cs to Au) elements including the Darwin relativistic effect.
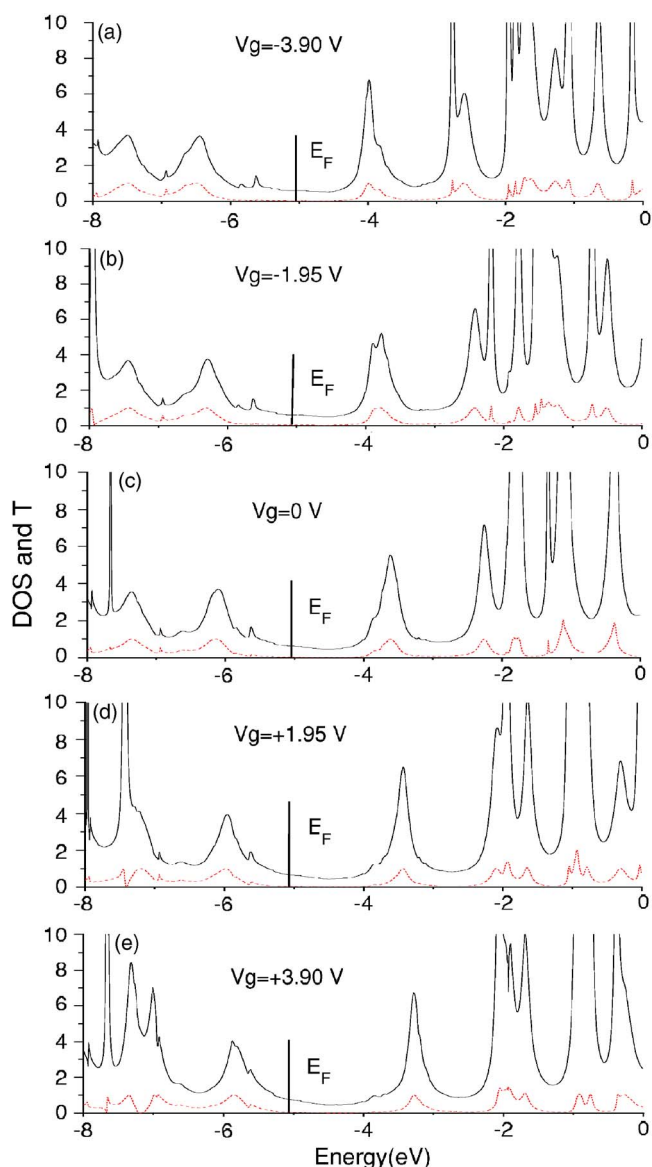

FIG. 2. (Color online) DOS (solid) and T (dashed) as functions of energy for PTA with gold contacts connected, with the transverse gate bias $V_g = -3.90$ V (a), -1.95 V (b), 0 V (c), +1.95 V (d), and +3.90 V (e). The vertical line denotes the position of the Fermi level.

III. RESULTS AND DISCUSSION

The calculated DOS and T of PTA with the different transverse gate biases are given in Fig. 2. The sulfur atom in thiophene is sp^2 hybridized, and its p orbital provides two electrons to the π system. The linearly condensed thiophene molecules possess the extended π conjugation and the high planarity. Of the cyclic single organic molecules, the thiophene-based compound is one of the promising classes of organic materials. PTA is attractive, due to the stability of the thiophene ring and the good planarity.[25] The position of the broadened levels in equilibrium for the open system is determined by the singular points of Green function, obtained from the equation $(F + \Sigma_1 + \Sigma_2)C = SC\lambda$. The molecular levels are modulated by the transverse gate bias applied to the molecule with highest occupied molecular orbital (HOMO) [lowest unoccupied molecular orbital (LUMO)] position at $-6.47[-3.93]$ eV for $V_g = -3.90$ V (a), -6.27
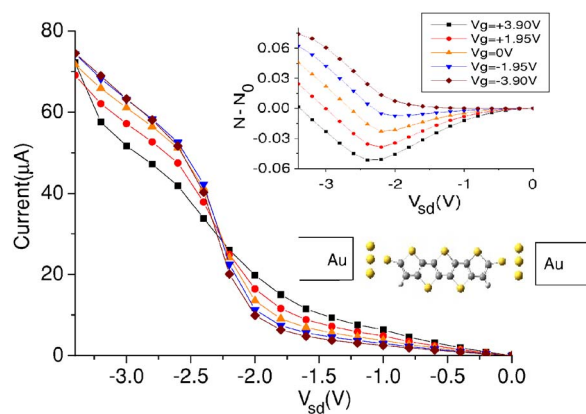
FIG. 3. (Color online) Gate modulation of the I-V characteristics for PTA. The $V_{sd}=-2.25$ V is the crossover point for the current controlled by the gate bias. For $V_{sd}>-2.25$ V, either electron ($V_g=-3.90$ V) or hole ($V_g \geq -1.95$ V) is responsible for the current. For -3.4 V$< V_{sd} < -2.25$ V, the molecule enters the electron and hole hybrid conduction region, and the positive biased current is smaller than the negative ones.

$[-3.77]$ eV for $V_g=-1.95$ V (b), $-6.09[-3.60]$ eV for $V_g=0$ V (c), $-5.93[-3.42]$ eV for $V_g=+1.95$ V (d), and $-5.79[-3.24]$ eV for $V_g=+3.90$ V (e). With the decrease of the positive gate bias, the separation between HOMO and Fermi level increases, and the separation between LUMO and Fermi level decreases. For the positive gate bias $V_g \geq 0$, the Fermi level is close to HOMO, and PTA is the p-type or hole conduction molecule, while for the big negative bias PTA is the n-type or electron conduction molecule. For large positive bias $V_g=+3.90$ V, the HOMO, close to E_F, contributes to the initial rise of the current under the small V_{sd} (1.0 V or so) in the longitudinal direction. In the case of large negative bias $V_g=-3.90$ V, LUMO is close to E_F and responsible for the molecular conduction. In Fig. 3 the gate bias successfully controls the I-V characteristics of the PTA. At the $V_{sd}>-2.25$ V, due to the contribution from HOMO, the positive gate bias achieves the bigger molecular current and at the $V_{sd}<-2.25$ V, as LUMO enters the V_{sd} window and contributes to the molecular conduction, the inverse order of current appears. The inset illustrates the α electron (with spin-up) number deviation from the equilibrium state as a function of V_{sd}. At $V_{sd}>-2.25$ V, for gate bias $V_g=-3.90$ V, the electron is responsible for the conduction ($N>N_0$) and electron number rises slowly, while for $V_g \geq -1.95$ V, the hole is responsible for the conduction ($N<N_0$), so the electron number descends (the electron flows out of the molecule to the lead). At $V_{sd}<-2.25$ V, the molecule enters the electron and hole hybrid conduction region, accompanying the rapid rise of electron number, which means that the electron contribution dominates the conduction. Both the TFE and charge effect have contributions to the I-V curves.

Similar to PTA, the good TFE is achieved by the other fused-ring thiophene molecules. Figures 4(a) and 4(b) show the I-V curves of the three-fused-ring thiophene and seven-fused-ring thiophene controlled by the gate bias. For example, at $V_{sd}=-1.0$ V, for the three-fused-ring thiophene molecules, $(I_{V_g=+1.95 \text{ V}}-I_{V_g=0 \text{ V}})/(I_{V_g=0 \text{ V}}) \doteq 0.14$, $(I_{V_g=+3.90 \text{ V}}-I_{V_g=0 \text{ V}})/(I_{V_g=0 \text{ V}}) \doteq 0.30$; for the seven-fused-ring
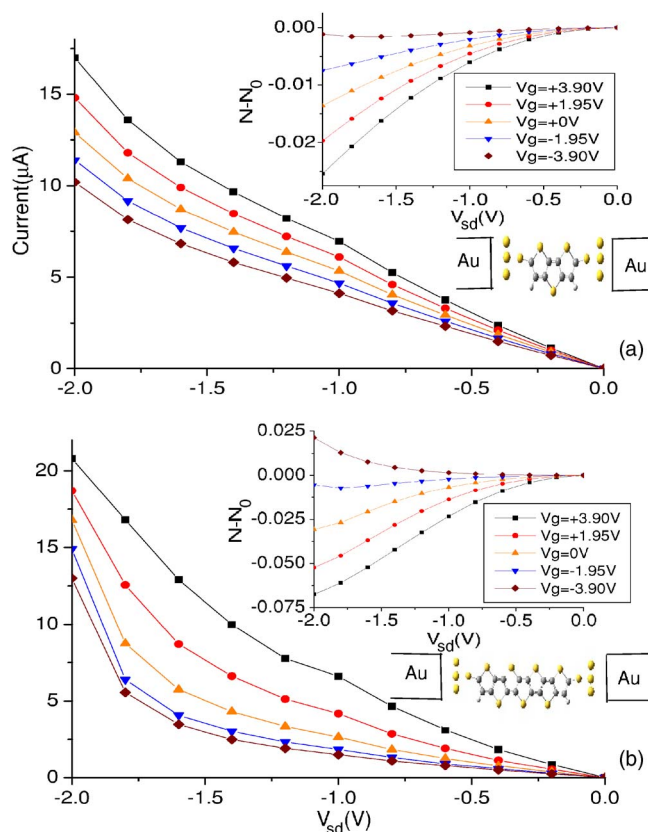
FIG. 4. (Color online) I-V curves of two fused-ring thiophenes corresponding to the different transverse fields: three-fused-ring thiophene (a) and seven-fused-ring thiophene (b). The inset shows the α electron number deviation from the equilibrium state with the modulation of bias.

thiophene, $(I_{V_g=+1.95 \text{ V}}-I_{V_g=0 \text{ V}})/(I_{V_g=0 \text{ V}}) \doteq 0.58$, $(I_{V_g=+3.90 \text{ V}}-I_{V_g=0 \text{ V}})/(I_{V_g=0 \text{ V}}) \doteq 1.49$. Meanwhile at the same source drain bias V_{sd} for PTA, $(I_{V_g=+1.95 \text{ V}}-I_{V_g=0 \text{ V}})/I_{V_g=0 \text{ V}} \doteq 0.29$, $(I_{V_g=+3.90 \text{ V}}-I_{V_g=0 \text{ V}})/I_{V_g=0 \text{ V}} \doteq 0.70$. The longer fused-ring thiophene molecules display a better TFE property.

The early experiment[36] reported only weak gate effect on the molecular current observed for the single benzene-dithiol molecule. Our calculation found that the TFE can be improved by the longer polyacene-dithiol molecules, which present a good transverse-field controlled molecular transistor. DOS and T of the single PDT, naphthalene-dithiol, and anthracene-dithiol in equilibrium without the longitudinal and transverse fields are shown in Fig. 5, where both HOMO and LUMO are close to E_F with increase in the aromatic phenyl ring. The HOMO (LUMO) is $-7.48(-2.75)$ eV for the single PDT, $-7.44(-3.55)$ eV for the naphthalene-dithiol, and $-6.98(-3.86)$ eV for the anthracene-dithiol. The fact predicts that if the number of aromatic phenyl ring is increased to more than 3, HOMO and LUMO will be closer to E_F, and the TFE will be more apparent. For the pentacene-dithiol, $|\text{HOMO}-\text{LUMO}| \doteq 2$ eV and E_F is almost in the middle of the HOMO-LUMO gap; it has apparent TFE in the small bias. The transmission peaks in the energy range within 1.0 eV below E_F come from the metal induced gap states (MIGS) which are the hybridization of HOMO state and metal surface state. The MIGS also can be found in Fig. 2.
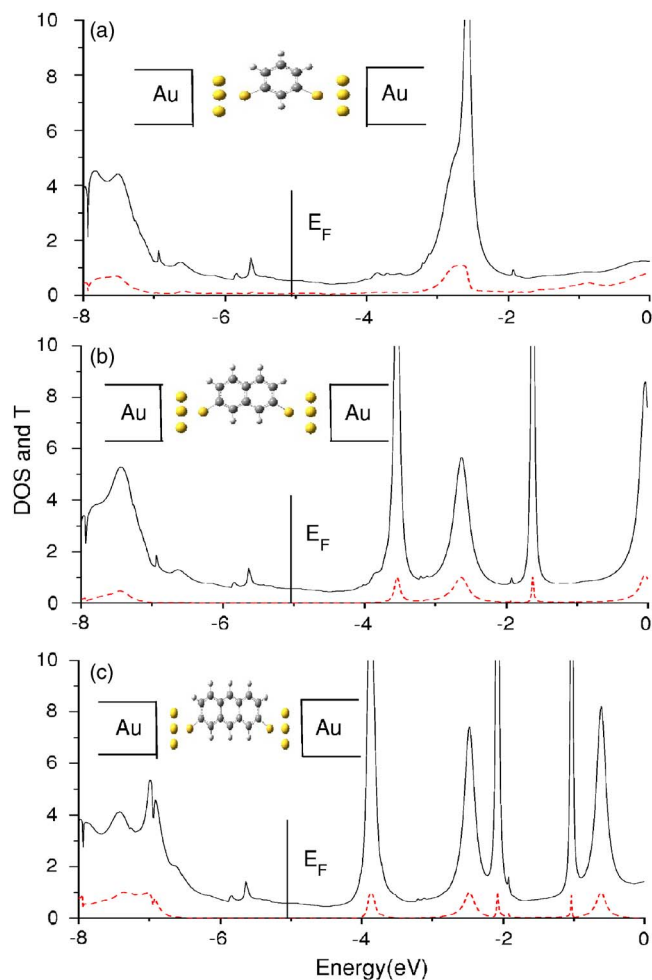
FIG. 5. (Color online) DOS (solid) and *T* (dashed) as functions of energy corresponding to the different aromatic phenyl ring molecules with gold contacts for single PDT (a), naphthalene-dithiol (b), and anthracene-dithiol (c). The vertical line denotes the position of the Fermi level.

The anthracene-dithiol is the *n*-type conduction molecule in the small V_{sd} region; its LUMO is closer to E_F than HOMO [see Fig. 5(c)]. Its molecular levels can be modulated obviously by the gate bias. With the gate bias increased from $V_g=-5.00$ V to $V_g=+5.00$ V by increments of 2.5 V, the HOMO of anthracene-dithiol leaves E_F by values of -6.17, -6.61, -6.98, -7.23, and -7.36 eV; and LUMO approaches E_F by values of -2.84, -3.34, -3.86, -4.37, and -4.83 eV, respectively.

With the gate bias $V_g=5.00$ V, the separation between E_F and LUMO, $|E_F-\text{LUMO}|=0.27$ eV, leads the large current at small V_{sd}. The *I-V* curves of anthracene-dithiol controlled by the gate bias are shown in Fig. 6. The current magnitude of the anthracene-dithiol is one order smaller than the one of the fused-ring thiophene molecules, which is in favor of the low-power devices. The molecular transistor illustrates the effective current separation under control of the positive gate bias. For $V_{sd}=-1.0$ V, $(I_{V_g=+2.50 \text{ V}} -I_{V_g=0 \text{ V}})/(I_{V_g=0 \text{ V}}) \doteq 0.61$, $(I_{V_g=+5.00 \text{ V}}-I_{V_g=0 \text{ V}})/(I_{V_g=0 \text{ V}}) \doteq 5.89$; while for $V_{sd}=-2.0$ V, $(I_{V_g=+2.50 \text{ V}}-I_{V_g=0 \text{ V}})/ (I_{V_g=0 \text{ V}}) \doteq 3.05$, $(I_{V_g=+5.00 \text{ V}}-I_{V_g=0 \text{ V}})/(I_{V_g=0 \text{ V}}) \doteq 9.14$. We notice that in the V_{sd} range from -1.0 to -2.0 V, the current under the transverse field of $V_g=-5.00$ V is bigger than that
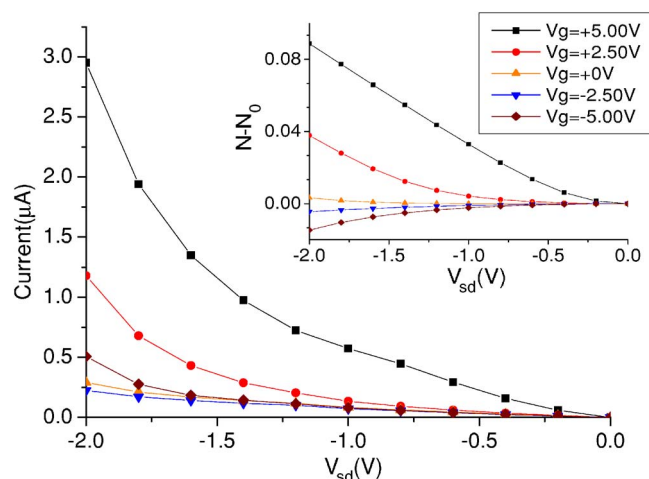

FIG. 6. (Color online) *I-V* curves of pentacene-dithiol corresponding to the different gate biases. The inset shows the α electron number deviation from the equilibrium state with the change of bias.

at $V_g=0$ V, which is not found for fused-ring oligothiophene molecules. The gate-controlled current separation for the negative bias is not effective; it is better to use the positive bias to control the molecular transistor. For the anthracene-dithiol, the transverse field of $V_g=-5.00$ V makes HOMO close to -6.0 eV, accompanying the sudden rise of current around $V_{sd}=-2.0$ V, so its current is larger than the one for $V_g=0$ V where neither HOMO nor LUMO enters the V_{sd} window. The inset of Fig. 6 illustrates the electron number deviation from equilibrium.

For the open system without the transverse bias, the α electron number has almost no variation below $V_{sd}=2.0$ V, since both HOMO and LUMO keep away from E_F in the V_{sd} range. With increase of gate bias, LUMO is shifted to E_F gradually, and the electrons entering the molecule are more than that leaving the molecule, which makes the electron number increase. With decrease of the bias, HOMO approaches E_F gradually, which makes the electron number decrease.

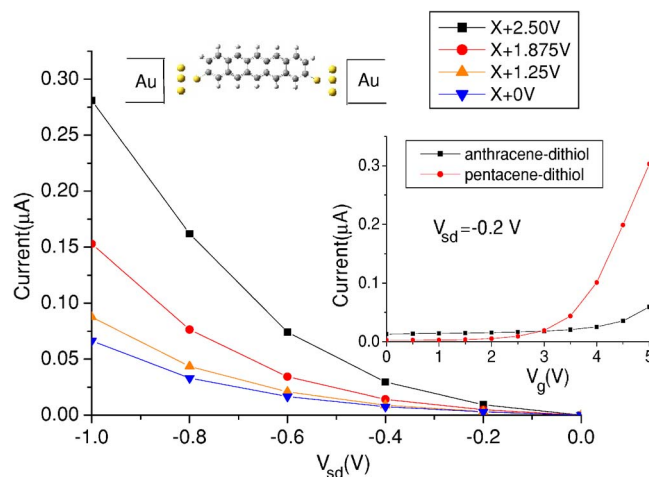With increase in the number of aromatic phenyl ring, the

FIG. 7. (Color online) *I-V* curves of anthracene-dithiol corresponding to the different gate biases. The inset shows the transfer characteristic curves of anthracene-dithiol and pentacene-dithiol corresponding to the $V_{sd}=-0.2$ V.
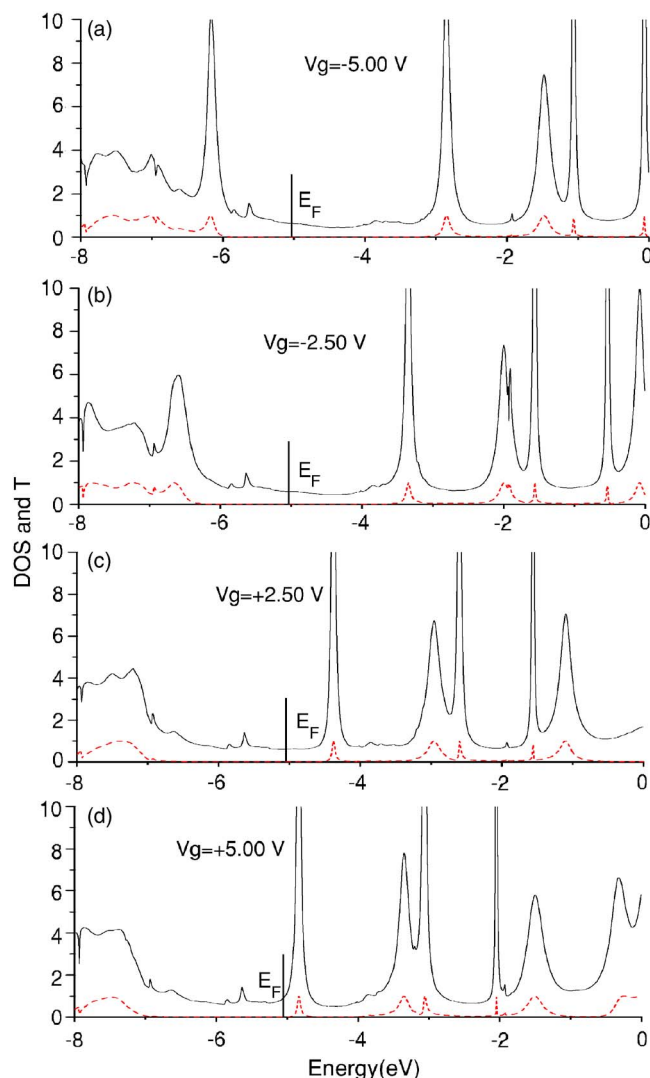
FIG. 8. (Color online) DOS (solid) and T (dashed) as functions of energy for anthracene-dithiol with gold contacts connected, with the transverse gate bias. $V_g = -5.0$ V (a), -2.5 V (b), $+2.5$ V (c), and $+5.0$ V (d). The vertical line denotes the position of the Fermi level.

TFE is improved. We found that TFE of the naphthalene-dithiol is better than that of the single PDT, but not better than that of the anthracene-dithiol. For the single PDT, under $V_{sd} = -1.0$ V, $(I_{V_g=+2.50\text{ V}} - I_{V_g=0\text{ V}})/(I_{V_g=0\text{ V}}) \doteq 0.03$, $(I_{V_g=+5.00\text{ V}} - I_{V_g=0\text{ V}})/(I_{V_g=0\text{ V}}) \doteq 0.11$, while under $V_{sd} = -2.0$ V, $(I_{V_g=+2.50\text{ V}} - I_{V_g=0\text{ V}})/(I_{V_g=0\text{ V}}) \doteq 0.04$, $(I_{V_g=+5.00\text{ V}} - I_{V_g=0\text{ V}})/(I_{V_g=0\text{ V}}) \doteq 0.12$. The control of the molecular current by the gate bias is not discernible, which is consistent with the experiment.[35] The I-V curves of the pentacene-dithiol under the different gate biases are shown in Fig. 7. Under $V_{sd} = -1.0$ V, the molecular device presents the obvious current modulation by the gate bias: $(I_{V_g=+1.25\text{ V}} - I_{V_g=0\text{ V}})/(I_{V_g=0\text{ V}}) \doteq 0.32$; $(I_{V_g=+1.875\text{ V}} - I_{V_g=0\text{ V}})/(I_{V_g=0\text{ V}}) \doteq 1.31$; $(I_{V_g=+2.50\text{ V}} - I_{V_g=0\text{ V}})/(I_{V_g=0\text{ V}}) \doteq 3.23$. The molecule illustrates the five times of the current modulation rate of the anthracene-dithiol under the same gate bias. The inset of Fig. 7 gives the transfer characteristic curves of anthracene-dithiol and pentacene-dithiol corresponding to $V_{sd} = -0.2$ V. It is clear that the switch gate bias ($V_{sw} = 4.0$ V) of anthracene-dithiol is bigger than that of pentacene-dithiol

($V_{sw} = 3.0$ V). Considering the stability of the structure, maybe the anthracene-dithiol is still a better candidate for the molecular transistor.

The above TFE comes from the fact that the increase in the transverse field will increase energy levels of the fused-ring thiophene (Fig. 2) and decrease energy levels of the polyacene-dithiol (Fig. 8).

IV. SUMMARY

We use the self-consistent method based on the DFT and nonequilibrium Green function to simulate molecular transport. In terms of GAUSSIAN03, the electronic structures of the molecular device and the macroscopic leads are calculated on an equal footing. At the same time, the self-consistent iteration cycle is extended from the local molecule to the open system, by inserting the calculation of the density matrix of the open system as a subroutine. Our self-consistent results show that the long-length organic molecule can achieve better transport characteristics. Our investigation proves that both the polyacene-dithiol molecules and fused-ring oligothiophene molecules can be made as the high-frequency molecular transistors controlled by the transverse field. The theoretical results suggest the related experiments about the molecular devices. In the future work, we will apply ourselves to looking for the I-V curves of single molecule similar to that of FET.

[1] A. Nitzan and M. A. Ratner, Science **300**, 1384 (2003).
[2] *Molecular Nanoelectronics*, edited by M. A. Reed and T. Lee (American Scientific Publishers, Stevenson Ranch, CA, 2003).
[3] M. A. Reed, C. Zhou, C. J. Muller, T. P. Burgin, and J. M. Tour, Science **278**, 252 (1997).
[4] D. I. Gittins, D. Bethell, D. J. Schriffrin, and R. J. Nichols, Nature (London) **408**, 67 (2000).
[5] X. D. Cui, A. Primak, X. Zarate, J. Tomfohr, O. F. Sankey, A. L. Moore, T. A. Moore, D. Gust, G. Harris, and S. M. Lindsay, Science **294**, 571 (2001).
[6] B. Larade, J. Taylor, Q. R. Zheng, H. Mehrez, P. Pomorski, and H. Guo, Phys. Rev. B **64**, 195402 (2001).
[7] N. B. Zhitenev, H. Meng, and Z. Bao, Phys. Rev. Lett. **88**, 226801 (2002).
[8] J. Park, A. N. Pasupathy, J. I. Goldsmith *et al.*, Nature (London) **417**, 722 (2002).
[9] W. Liang, M. P. Shores, M. Bockrath, J. R. Long, and H. Park, Nature (London) **417**, 725 (2002).
[10] R. H. M. Smit, Y. Noat, C. Untiedt, N. D. Lang, M. C. van Hemert, and J. M. van Ruitenbeek, Nature (London) **419**, 906 (2002).
[11] J. Reichert, R. Ochs, D. Beckmann, H. B. Weber, M. Mayor, and H. v. Löhneysen, Phys. Rev. Lett. **88**, 176804 (2002).
[12] R. H. M. Smit, C. Untiedt, G. Rubio-Bollinger, R. C. Segers, and J. M. van Ruitenbeek, Phys. Rev. Lett. **91**, 076805 (2002).
[13] D. Dulic, S. J. van der Molen, T. Kudernac, H. T. Jonkman, J. J. D. de Jong, T. N. Bowden, J. van Esch, B. L. Feringa, and B. J. van Wees, Phys. Rev. Lett. **91**, 207402 (2003).
[14] B. Xu and N. J. Tao, Science **301**, 1221 (2003).

[15] B. Xu, X. Xiao, and N. J. Tao, J. Am. Chem. Soc. **125**, 16164 (2003).

[16] X. Xiao, B. Xu, and N. J. Tao, Nano Lett. **4**, 267 (2003).

[17] H. G. Heller, IEE Proc., Part I: Solid-State Electron Devices **130**, 209 (1983).

[18] Z. F. Liu, K. Hashimoto, and A. Fujishima, Nature (London) **347**, 658 (1990).

[19] P. E. Kornilovitch, A. M. Bratkovsky, and R. S. Williams, Phys. Rev. B **66**, 245413 (2002).

[20] M. A. Reed and J. M. Tour, Sci. Am. **282**(6), 86 (2000).

[21] J. P. Parakka, R. R. Schumaker, J. D. Thoburn, B. S. Kesler, and S. E. Branz, Ann. N.Y. Acad. Sci. **1006**, 94 (2003).

[22] Y. Chen, G.-Y. Jung, D. A. A. Ohlberg, X. Li, D. R. Stewart, J. O. Jeppesen, K. A. Nielsen, J. FraserStoddart, and R. S. Williams, Nanotechnology **14**, 462 (2003).

[23] P. J. Kuekes, D. R. Stewart, and R. S. Williams, J. Appl. Phys. **97**, 034031 (2005).

[24] C. Zhang, M.-H. Du, H.-P. Cheng, X.-G. Zhang, A. E. Roitberg, and J. L. Krause, Phys. Rev. Lett. **92**, 158301 (2004).

[25] K. Xiao, Y. Liu, T. Qi *et al.*, J. Am. Chem. Soc. **127**, 13281 (2005).

[26] Y. Sun, Y. Liu, and D. Zhu, J. Mater. Chem. **15**, 53 (2005).

[27] B. Xu, X. Xiao, X. Yang, L. Zang, and N. Tao, J. Am. Chem. Soc. **127**, 2386 (2005).

[28] E. Emberly and G. Kirczenow, J. Appl. Phys. **88**, 5280 (2000).

[29] M. Di Ventra, S. T. Pantelides, and N. D. Lang, Appl. Phys. Lett. **76**, 3448 (2000).

[30] Z. Q. Yang, N. D. Lang, and M. Di Ventra, Appl. Phys. Lett. **82**, 1938 (2003).

[31] A. Ghosh, T. Rakshit, and S. Datta, Nano Lett. **4**, 565 (2004).

[32] P. S. Damle, A. W. Ghosh, and S. Datta, Chem. Phys. **281**, 171 (2002).

[33] F. Jiang, Y. X. Zhou, H. Chen, R. Note, H. Mizuseki, and Y. Kawazoe, Phys. Rev. B **72**, 155408 (2005).

[34] D. Papaconstantopoulos, *Handbook of the Band Structure of Elemental Solids* (Plenum, New York, 1986).

[35] M. J. Frisch, G. W. Trucks, H. B. Schlegel *et al.*, GAUSSIAN 03, Revision B.04 (Gaussian, Inc., Pittsburgh, PA, 2003).

[36] J.-O. Lee, G. Lientschnig, F. Wiertz, M. Struijk, R. A. J. Janssen, R. Egberink, D. N. Reinhoudt, P. Hadley, and C. Dekker, Nano Lett. **3**, 113 (2003).